Supplemental Figures

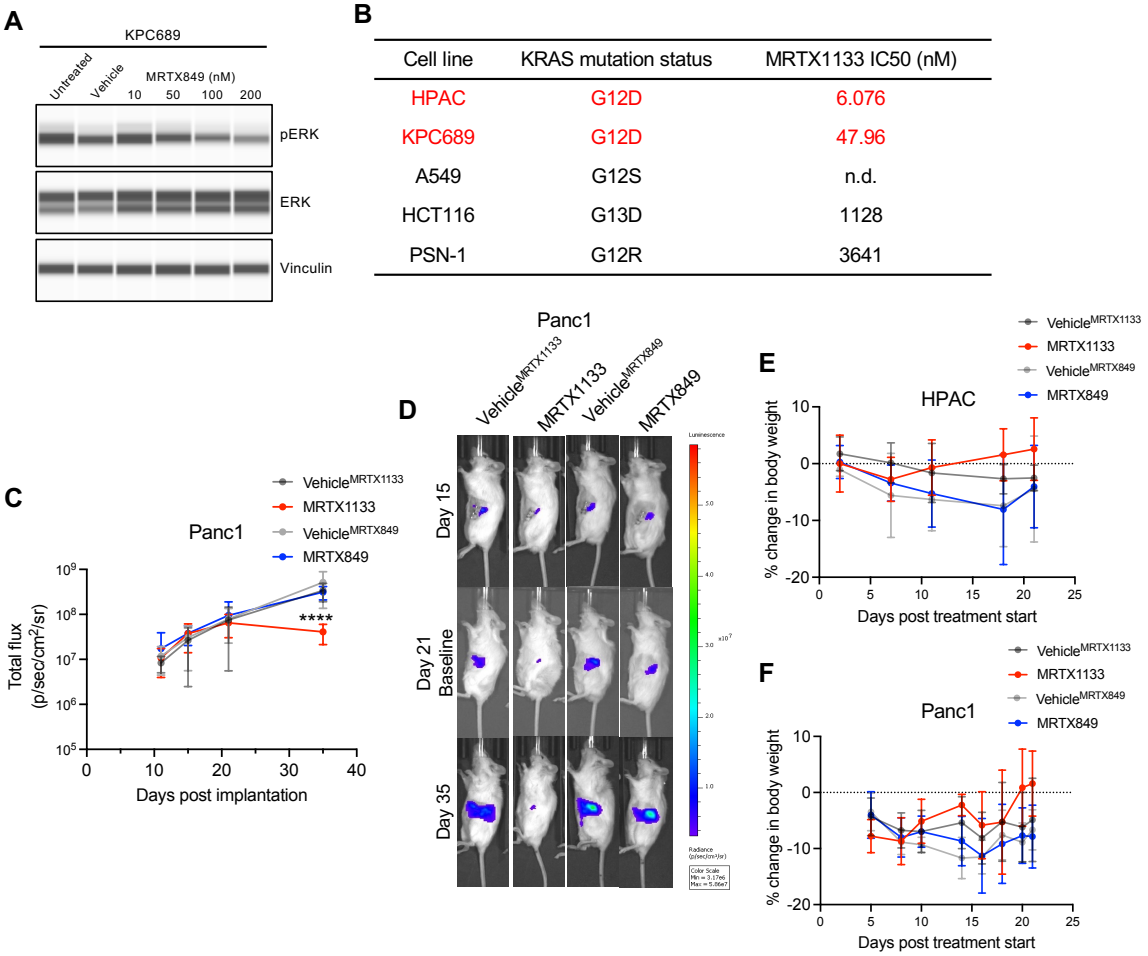

Figure S1: Specificity of MRTX1133 and efficacy in human xenograft models, related to Figure 1. (**A**) Capillary immunoassay for pERK and vinculin abundance in KPC689 cells in response to MRTX849. Vehicle: DMSO. (**B**) Calculated MRTX1133 IC50 values for the listed cell lines and Kras mutation status. (**C**) Bioluminescence of Panc1 tumors over time. Treatment started at day 21 (Vehicle^{MRTX1133}: n=5, MRTX1133: n=10, Vehicle^{MRTX849}: n=5, MRTX849: n=10). (**D**) Representative bioluminescence images of Panc1 tumors. (**E-F**) Change in body weight of mice with HPAC (Vehicle^{MRTX1133}: n=5, MRTX1133: n=10, Vehicle^{MRTX849}: n=5, MRTX849: n=10) (**E**) or Panc1 (Vehicle^{MRTX1133}: n=5, MRTX1133: n=10, Vehicle^{MRTX849}: n=5, MRTX849: n=10) (**F**) post-treatment start. In **C, E and F**, data are presented as mean ± SD. Significance was determined by two-way ANOVA with Sidak's multiple comparisons in **C**.*** P<0.001.

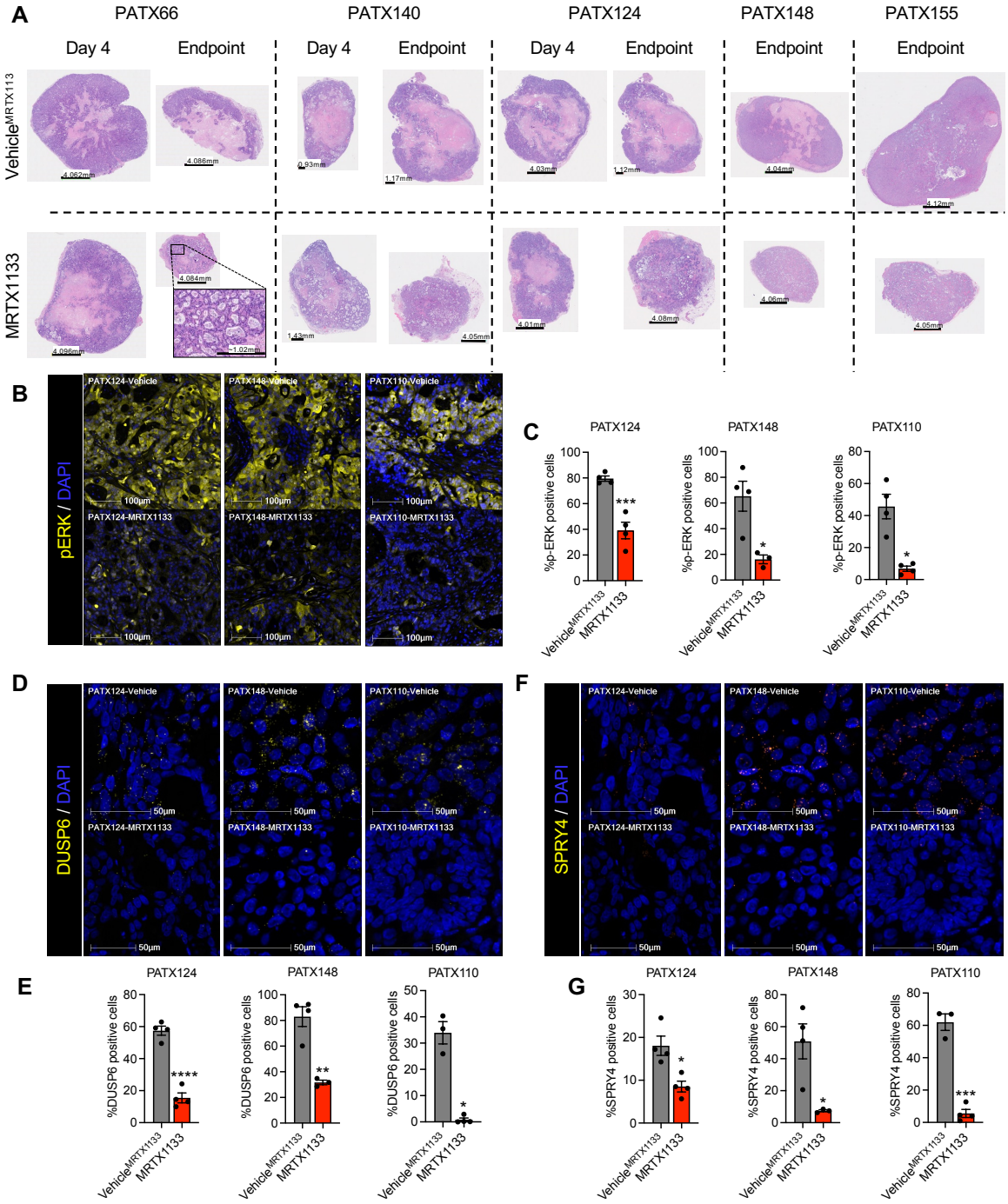

Figure S2: Target engagement in MRTX1133 treated PDXs, related to Figure 1. (**A**) Representative H&E stained pancreas/tumors from the listed PDXs and treatment. **(B-C)** Representative pERK immunostaining (**B**) and quantification (**C**) in indicated PDXs (n=3-4/group). Scale bar, 100 μm. **(D-E)** Representative *DUSP6* RNA in situ hybridization (ISH) staining (**D**) and quantification (**E**) in indicated PDXs (n=3-4 per group). Scale bar, 50 μm. **(F-G)** Representative

SPRY4 RNA ISH staining (**F**) and quantification (**G**) of indicated PDXs (n=3-4 per group). Scale bar, 50 μm. Significance was determined by unpaired t-test in **C, E** and **G**. Welch's correction was used for PATX110 in **C**, PATX110 in **E** and PATX148 in **G**. * P<0.05, ** P<0.01, *** P<0.001, **** P<0.0001, *ns*: not significant.

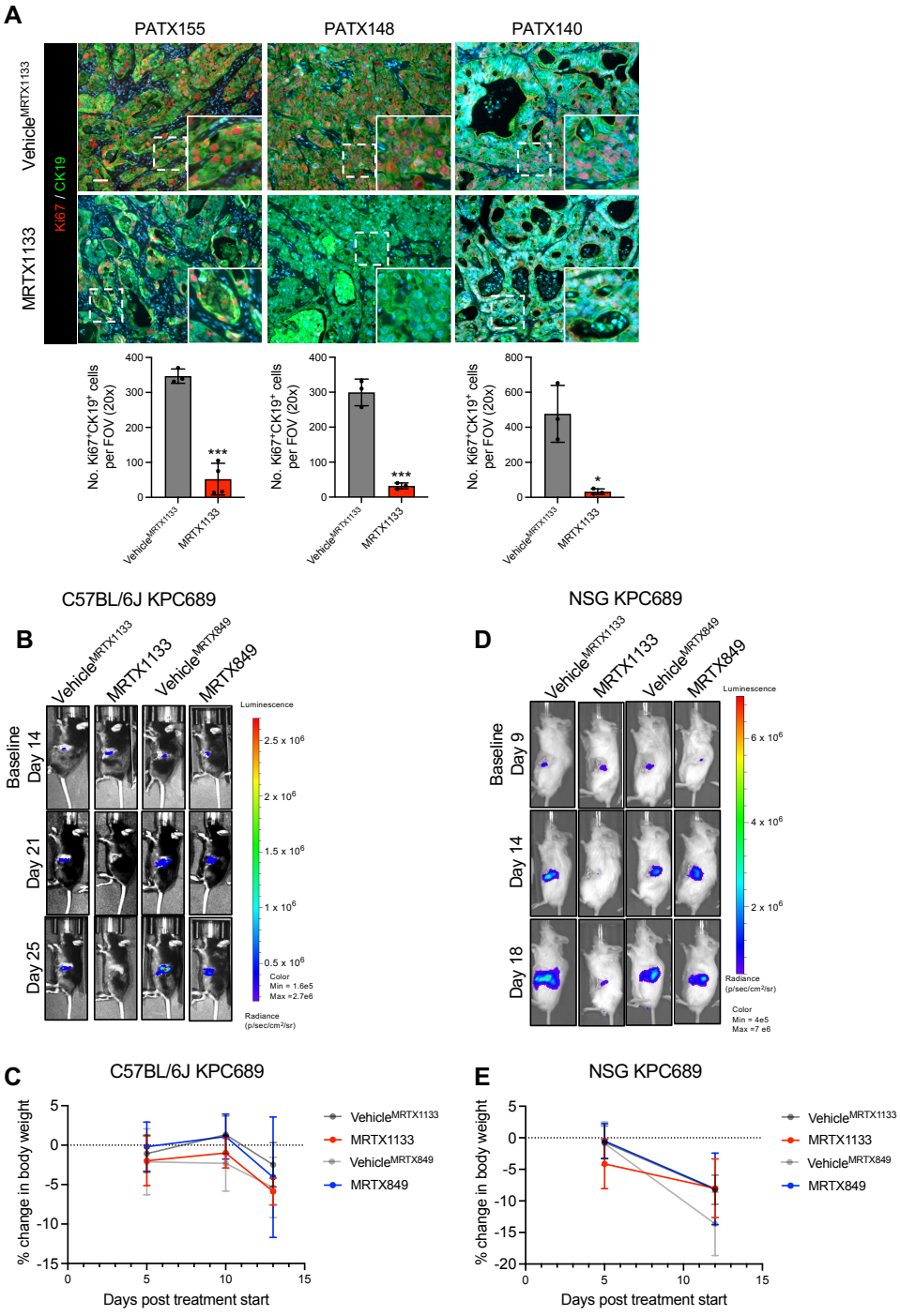

Figure S3: Inhibition of proliferation in PDXs, bioluminescence of KPC689 tumors and body weight measurements, related to Figures 1 and 2. (**A**) Representative images of Ki67 and CK19 immunostaining and quantification of proliferative cancer cells (Ki67^{+}CK19^{+} cells) of the indicated PDXs. Scale bar, 50 μm. (**B-C**) Representative bioluminescence images (**B**) and change in body weight (**C**) of C57BL/6J mice with orthotopic KPC689 tumors (Vehicle^{MRTX1133}:

n=5, MRTX1133: n=9, Vehicle^{MRTX849}: n=5, MRTX849: n=9). (**D-E**) Representative bioluminescence images (**D**) and change in body weight (**E**) of NSG mice with orthotopic KPC689 tumors (Vehicle^{MRTX1133}: n=5, MRTX1133: n=9, Vehicle^{MRTX849}: n=5, MRTX849: n=10). Data are presented as mean $\pm$ SD in **A, C,** and **E**. Unpaired t-test performed for PATX155 and PATX148 and Welch's t-test performed for PATX140 in **A**. * $P<0.05$, *** $P<0.001$.

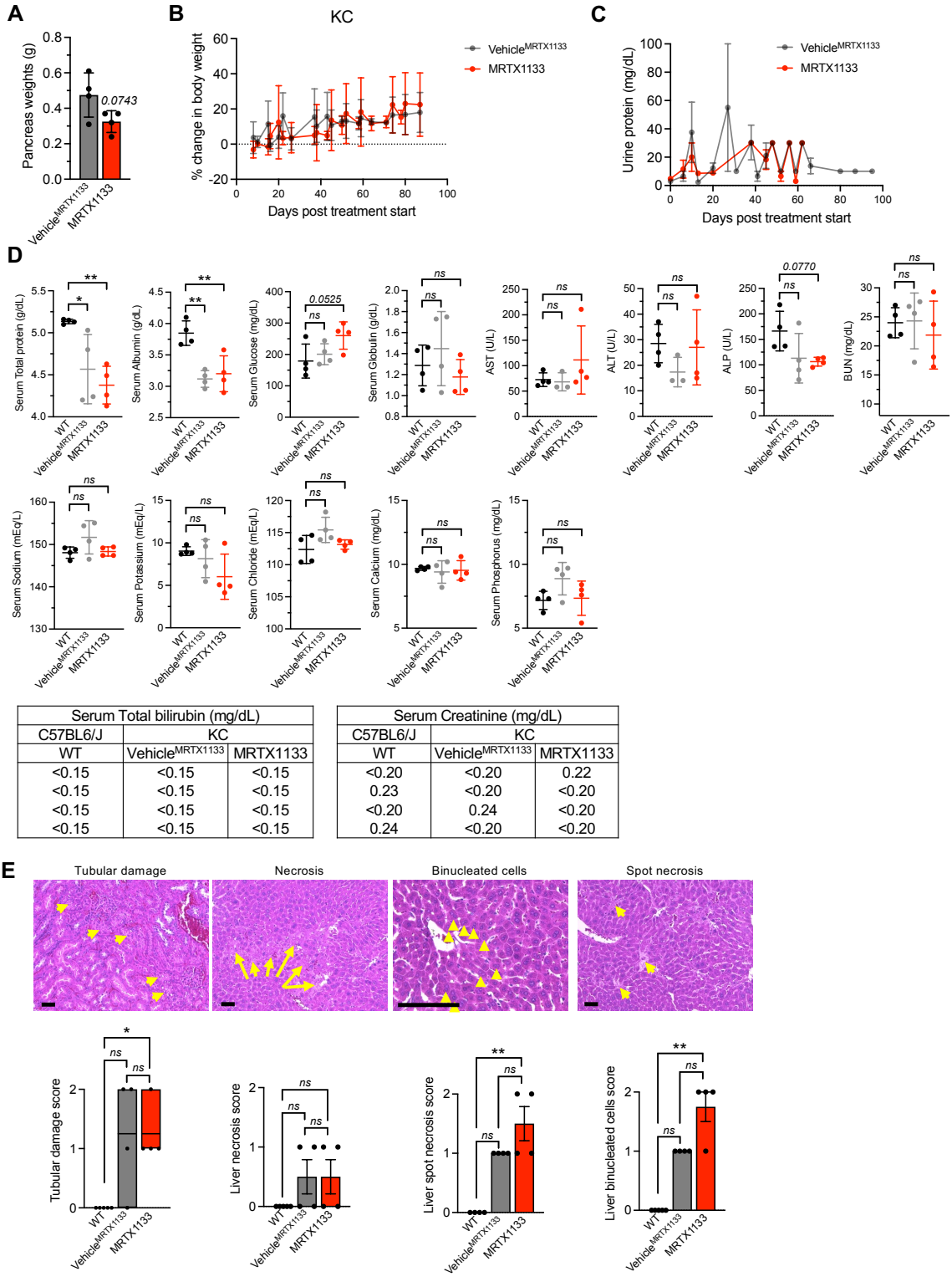

Serum Total bilirubin (mg/dL)		
C57BL6/J	KC	
WT	Vehicle^{MRTX1133}	MRTX1133
<0.15	<0.15	<0.15
<0.15	<0.15	<0.15
<0.15	<0.15	<0.15
<0.15	<0.15	<0.15

Serum Creatinine (mg/dL)		
C57BL6/J	KC	
WT	Vehicle^{MRTX1133}	MRTX1133
<0.20	<0.20	0.22
0.23	<0.20	<0.20
<0.20	0.24	<0.20
0.24	<0.20	<0.20

Figure S4: KRAS* inhibition is not associated with toxicity in spontaneous KC mice, related to Figure 3. (**A**) Pancreata weight at endpoint (20 weeks) of spontaneous KC mice (n=4 per

group). Exact p-value is reported. (**B**) Change in body weight of spontaneous KC mice post-treatment start (n=9 per group). (**C**) Measurement of protein in urine during treatment of spontaneous KC mice (n=9 per group). (**D**) Blood chemistry analysis at endpoint (20 weeks) of spontaneous KC mice (n=4 per group). (**E**) Representative H&E images (top) and scoring (bottom) of kidney tubular damage, liver necrosis, liver binucleated cells, and spot necrosis. Arrows denote indicated types of tissue damage. In **A, B, C, D** and second, third, and fourth panels of **E**, data are presented as mean $\pm$ SD. In the left panel of **E**, data are presented with bars at the min, mean, and max. Significance was determined by unpaired t-test in **A**, Kruskal–Wallis with Dunn's multiple comparisons test **E**. In **D**, Kruskal–Wallis with Dunn's multiple comparisons test was used for AST and ALT panels and one-way ANOVA with Dunnett's multiple comparisons test for all other panels. Scale bar, 25 μm. * $P<0.05$, ** $P<0.01$, *ns*: not significant.

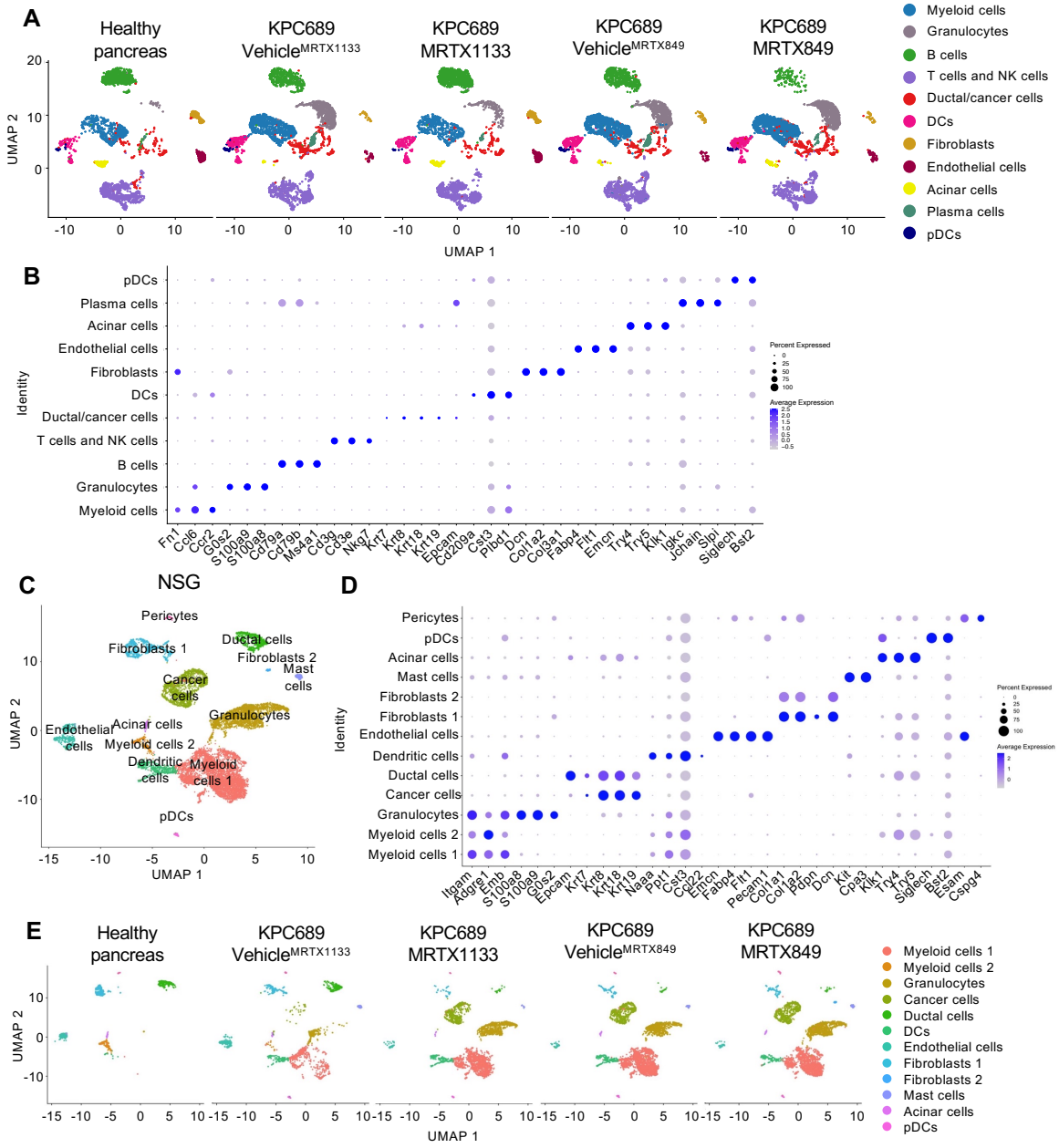

Figure S5: scRNA-seq analysis of KPC689 tumors in C57BL6/J mice and NSG mice, related to Figure 4. (**A-B**) UMAPs (**A**) and dot plot of genes used to define the cell types (**B**) in orthotopic KPC689 tumors in C57BL6/J mice determined by scRNA-seq analysis. (**C-E**) UMAP of all cells (**C**), dot plot of genes used to define the cell types (**D**), and UMAPs of individual tumors (**E**) of orthotopic KPC689 tumors in NSG mice determined by scRNA-seq analysis.

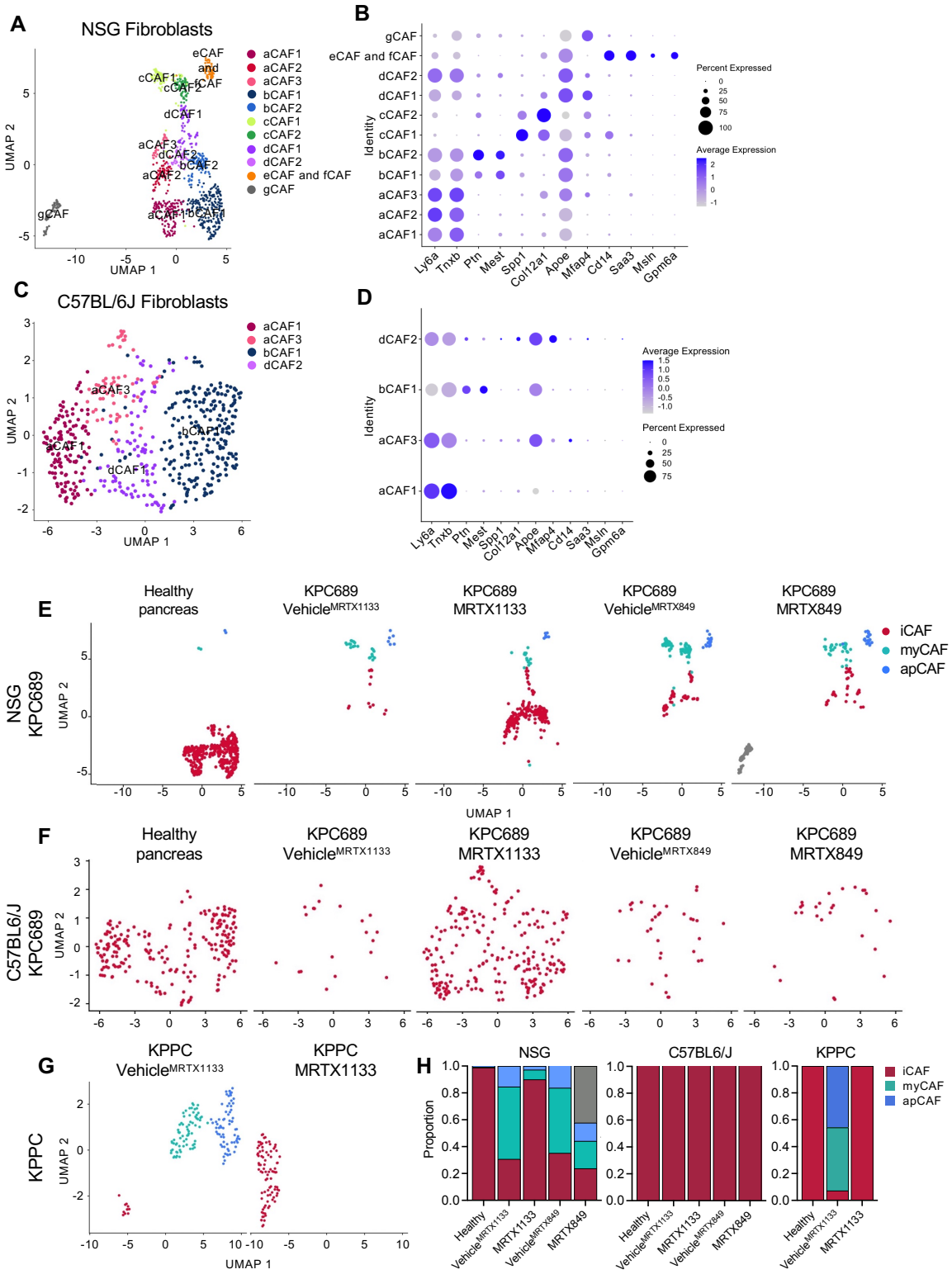

Figure S6: scRNA-seq analysis of fibroblasts in orthotopic KPC689 and spontaneous KPPC tumors, related to Figure 4. (**A-B**) UMAPs (**A**) and dot plot of genes associated with

fibroblast clusters (**B**) in orthotopic KPC689 tumors in NSG mice determined by scRNA-seq analysis. (**C-D**) UMAPs (**C**) and dot plot of genes associated with fibroblast clusters (**D**) in orthotopic KPC689 tumors in C57BL6/J mice determined by scRNA-seq analysis. (**E-G**) UMAPs of iCAF/myCAF/apCAF clustering in orthotopic KPC689 tumors in NSG mice (**E**), orthotopic KPC689 tumors in NSG mice (**F**), and spontaneous KPPC tumors (**G**). (**H**) Relative proportions of fibroblast subsets in orthotopic KPC689 tumors in NSG mice and C57BL6/J mice, and spontaneous KPPC tumors. Healthy for C57BL6/J and KPPC is the same sample as healthy controls were analyzed at the same time for both groups.

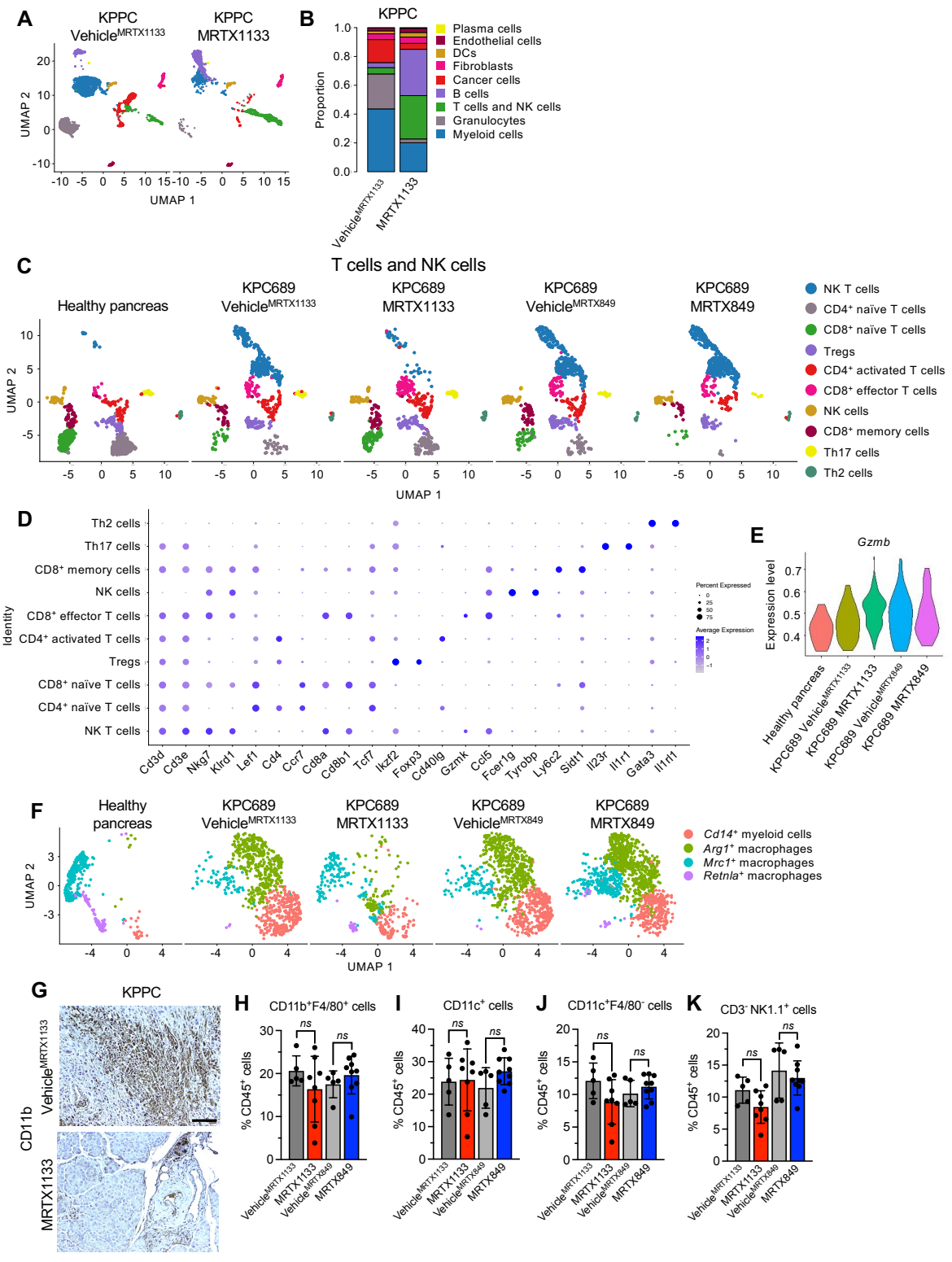

Figure S7: Analysis of immune infiltrate in response to KRAS* inhibition, related to Figure 5. (A-B) UMAPs (**A**) and proportion of cell types (**B**) in KPPC tumors.

(**C-D**) UMAPs (**C**) and dot plot of genes used to define T cells and NK cell subtypes (**D**) in orthotopic KPC689 tumors in C57BL6/J mice determined by scRNA-seq analysis. (**E**) Violin plot for *Gzmb* expression in $CD8^+$ effector T cells in orthotopic KPC689 tumors in C57BL6/J mice determined by scRNA-seq. (**F**) UMAPs of myeloid cell clusters in orthotopic KPC689 tumors in C57BL6/J mice determined by scRNA-seq analysis. (**G**) Representative images of CD11b immunostained spontaneous KPPC tumors. Scale bar, 100 μm. (**H-K**) Immunotyping of $CD11b^+F4/80^+$ (**H**), $CD11c^+$ (**I**), $CD11c^+F4/80^-$ (**J**), and $CD3^-NK1.1^+$ (**K**) immune cells by flow cytometry of orthotopic KPC689 tumors in C57BL6/J mice. $Vehicle^{MRTX1133}$: n=5, MRTX1133: n=8, $Vehicle^{MRTX849}$: n=5, MRTX849: n=9. Data are presented as mean $\pm$ SD in **H-K** and as violin plots in **E**. Significance was determined by unpaired t-test in **H-K** and for $Vehicle^{MRTX1133}$ vs. MRTX1133 comparisons in **H** and **I**. Mann-Whitney test was used for all other comparisons in **H** and **I**. *ns*: not significant.

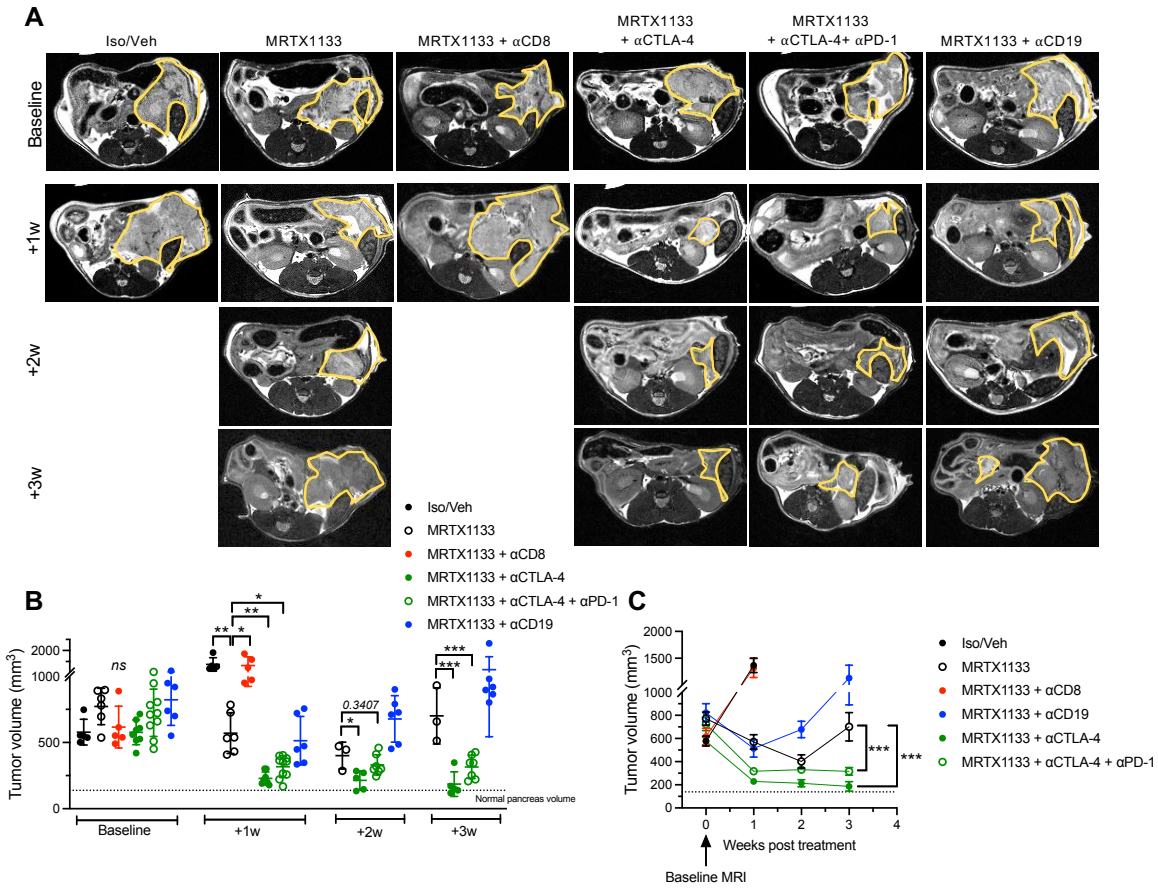

Figure S8: Growth kinetics of PKC-HY19636 orthotopic tumors, related to Figure 5. (**A-C**) MRI (**A**) tumor volume measurements and quantification (**B** and **C**) of indicated groups ((Iso/Veh (n=5), MRTX1133 (n=6), MRTX1133+αCD8 (n=5), MRTX1133+αCTLA-4 (n=6), MRTX1133+αCTLA-4+αPD-1 (n=10), MRTX1133+αCD19 (n=6)). Data are presented as mean ± SD in **B** and **C**. One-way ANOVA with Dunnett's multiple comparison test performed for baseline, 2 weeks, and 3 weeks, and Brown-Forsythe ANOVA with Dunnett's T3 multiple comparisons test performed for 1 week in **B-C**. Data are also presented in Fig. 5J and 5L and presented again here for direct comparison of tumor volume over time. * P<0.05, ** P<0.01, *** P<0.001, **** P<0.0001, *ns*: not significant.

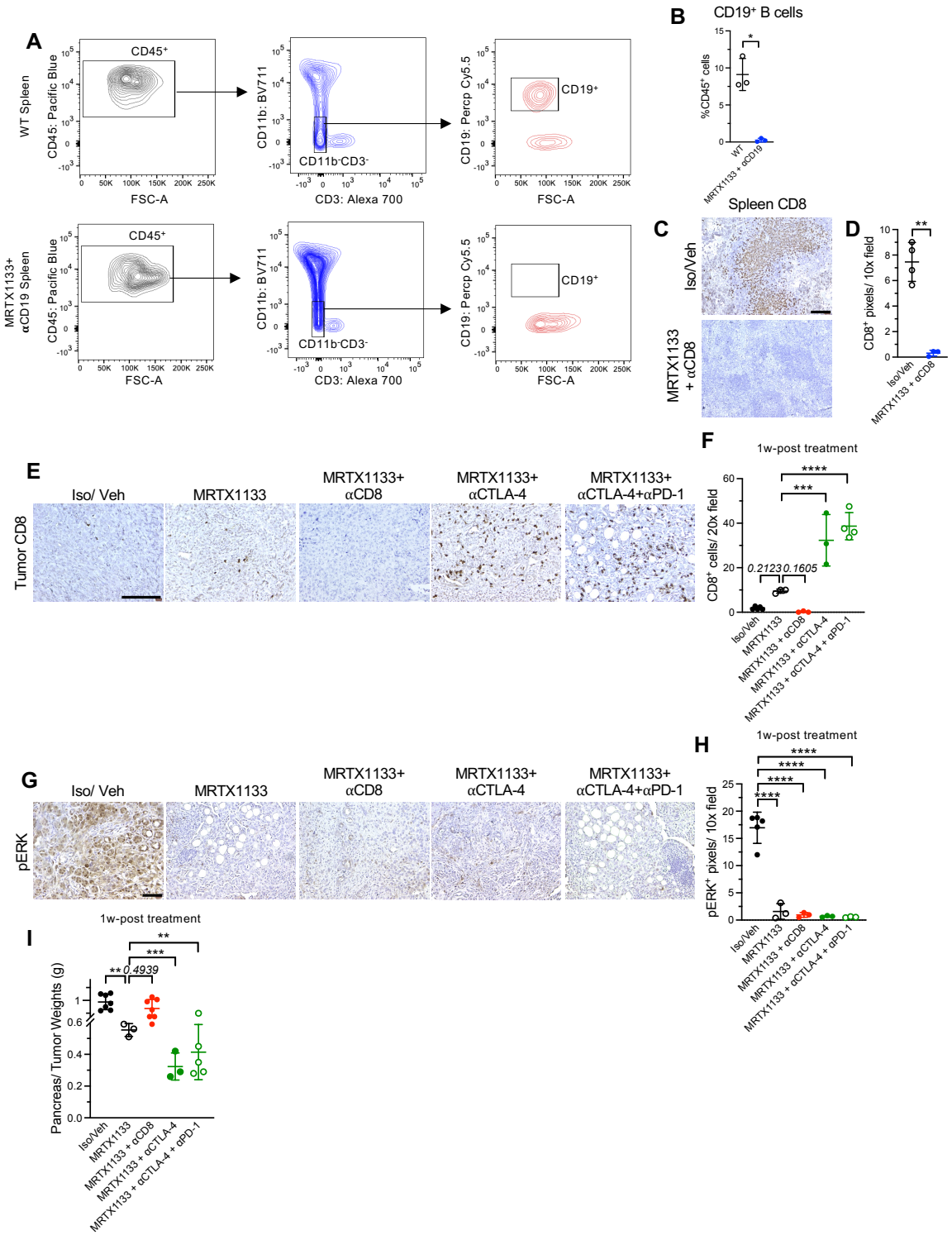

Figure S9: Confirmation of CD19$^+$ and CD8$^+$ cell depletion and MRTX1133 target engagement in PKC-HY19636 tumors, related to Figure 5. (**A-B**) Flow cytometry gating strategy **(A)** and quantification **(B)** of CD3$^-$CD11b$^-$CD19$^+$ B cells in the spleen of indicated groups

measured as a percentage of % $CD45^+$ cells (n=3 mice per group). **(C-D)** Representative CD8 IHC **(C)** and quantification **(D)** of spleen from Iso/Veh (n=4) and MRTX1133 + αCD8 (n=3) treated mice showing $CD8^+$ T cell depletion. **(E-F)** Representative CD8 immunostaining images **(E)** with quantification **(F)** of intra-tumoral $CD8^+$ T cells in indicated groups (Iso/Veh (n=5), MRTX1133 (n=3), MRTX1133+αCD8 (n=3), MRTX1133+αCTLA-4 (n=3), MRTX1133+αCTLA-4+ αPD-1 (n=4)). **(G-H)** Representative pERK immunostained images **(G)** and quantification **(H)** in indicated groups (n=3-4 per group). **(I)** Pancreas/tumor weights of age match euthanized mice (1 week post treatment) of indicated groups (Iso/Veh (n=7), MRTX1133 (n=3), MRTX1133+αCD8 (n=7), MRTX1133+αCTLA-4 (n=3), MRTX1133+αCTLA-4+ αPD-1 (n=5)). Data are presented as mean ± SD in **B, D, F, H** and **I**. Significance was determined by Welch's t-test in **B** and **D**, one-way ANOVA with Dunnett's multiple comparisons test in **F** and **H** and Brown-Forsythe ANOVA with Dunnett's T3 multiple comparisons test in **I**. Scale bars: 100 μm. * P<0.05, ** P<0.01, *** P<0.001, **** P<0.0001.

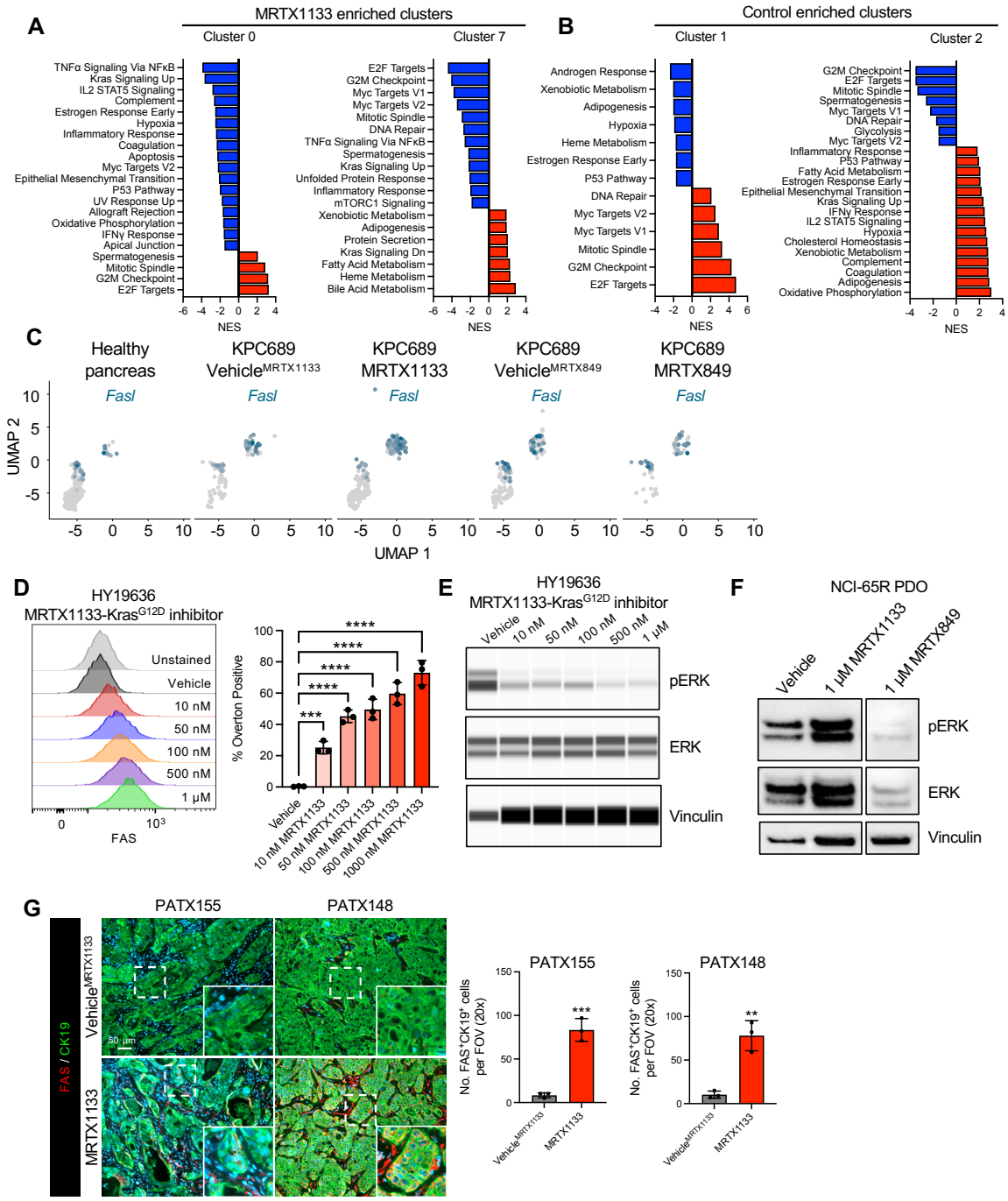

Figure S10: Upregulation of immune-related pathways and FAS in response to KRAS* inhibition, related to Figure 6. (**A-B**) GSEA of MRTX1133 enriched clusters (**A**) and control enriched clusters (**B**) determined by scRNA-seq analysis of KPC689 cells treated in vitro. Pathways reported with an FDR q-value < 0.1. NES: normalized enrichment score. (**C**) UMAPs of *Fasl* expression in CD8$^+$ T cells in orthotopic KPC689 tumors in C57BL6/J mice determined by

scRNA-seq analysis. (**D**) Representative flow plots and quantification of FAS expression in response to vehicle (DMSO) or the indicated concentrations of MRTX1133 in HY19636 cells. n=3 biological replicates per group. (**E**) pERK and total ERK in HY19636 at 24 hours post-treatment with vehicle (DMSO) or the indicated concentrations of MRTX1133. (**F**) pERK, total ERK, and vinculin abundance at 24 hours post-treatment of NCI-65R PDO with MRTX1133 or MRTX849 at the indicated concentrations. (**G**) Representative images of FAS and CK19 immunostaining and quantification of the indicated PDXs. Scale bar, 50 μm. Data are presented as mean ± SD in **D** and **G**. One-way ANOVA with Dunnett's multiple comparison test performed in **D**. Unpaired t-test performed in **G**. ** P<0.01, *** P<0.001, **** P<0.0001.

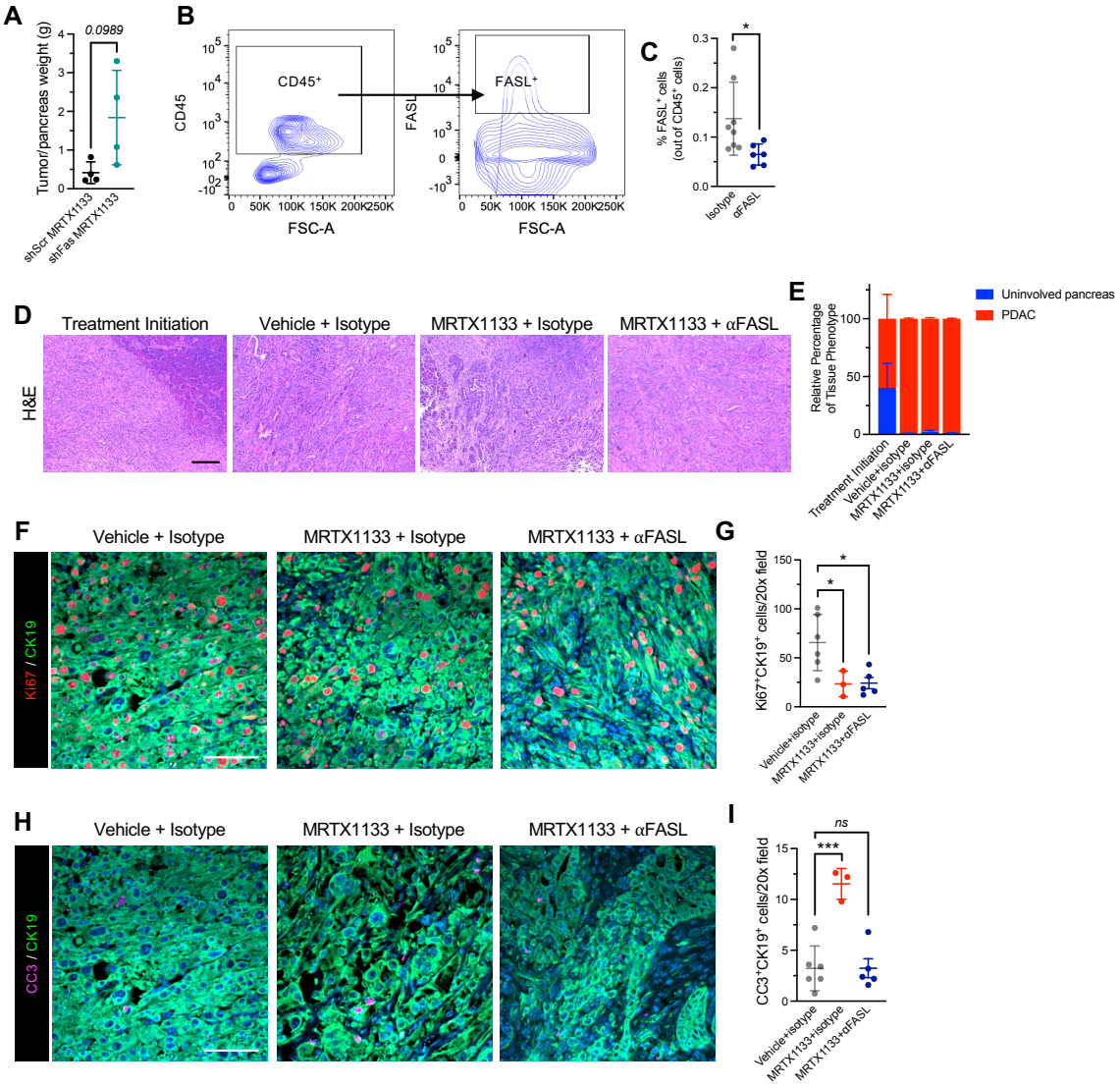

Figure S11: FAS silencing or FASL inhibition with KRAS* inhibition promotes PDAC tumor growth, related to Figure 7. (**A**) Pancreas/tumor weights of AK14837 tumors (shScr MRTX1133, n=4; shFas MRTX1133, n=4). (**B-C**) Flow cytometry gating strategy (**B**) and quantification (**C**) of FASL$^+$ cells out of CD45$^+$ cells in the spleen (Isotype, n=8; αFASL, n=6). (**D-E**) Representative H&E images (**D**) and associated histological scoring of KPC689 tumors (Treatment initiation, n=4; Vehicle+isotype, n=8; MRTX1133+Isotype, n=5; MRTX1133+αFASL, n=8) (**E**). (**F-G**) Representative images of Ki67 (red) and CK19 (green) immunostained KPC689 tumors (**F**) and quantification of Ki67$^+$CK19$^+$ cells (**G**) (Vehicle+isotype, n=6; MRTX1133+isotype, n=3; MRTX1133+αFASL, n=5). (**H-I**) Representative images of cleaved caspase 3 (CC3, pink) and CK19 (green) immunostained KPC689 tumors (**H**) and quantification of CC3$^+$CK19$^+$ cells (**I**)

(Vehicle+isotype, n=6; MRTX1133+isotype, n=3; MRTX1133+αFASL, n=5). Scale bars, 100 μm. Mann-Whitney t-test performed in **C**. Two-way ANOVA with Tukey's multiple comparison test performed for (**E**). One-way ANOVA with Dunnett's multiple comparison test performed for (**G**) and (**I**). * P<0.05, *** P<0.001, *ns*: not significant.

Supplemental Tables

Table S1: Cell lines and culture conditions. Related to STAR Methods.

Cell line	Origin	Media
HPAC	ATCC	DMEM/F12 (Corning), 5% FBS (Gemini), 0.002 mg/mL insulin (Sigma Aldrich), 0.005 mg/mL transferrin (Sigma Aldrich), 40 ng/mL hydrocortisone (Sigma Aldrich), 10 ng/mL EGF (Peprotech), 1% penicillin-streptomycin (P/S)
Panc1	ATCC	RPMI (Corning), 10% FBS, 1% P/S
A549	ATCC	DMEM (Corning), 10% FBS, 1% P/S
HCT116	ATCC	McCoy's-5A (Corning), 10% FBS, 100 mM L-glutamine, 1% NEAA, 1% P/S
PSN-1	ATCC	RPMI, 10% FBS, 1% P/S
MIA PaCa-2	ATCC	RPMI, 10% FBS, 1% P/S
KPC689	[32,33]	RPMI, 10% FBS, 1% P/S
PKC-HY19636	[34]	DMEM, 10% FBS, 1% P/S
AK14837	[4]	DMEM, 10% Tet-free FBS (Clontech), 1% P/S, 10 µg/mL puromycin (Sigma Aldrich), 1 µg/mL doxycycline (Sigma Aldrich)

Table S2: Patient derived xenografts (PDX). Related to STAR Methods.

PDX ID	Age/Gender	Patient tumor site	Known mutations
PATX124	63/M	Pancreatic head tumor	*KRAS^{G12D}, TP53^{R333Vfs*12}*
PATX148	75/M	Liver metastasis	*KRAS^{G12D}, TP53^{F134L}*
PATX140	72/M	Pancreatic head tumor	*KRAS^{G12D}, TP53^{G245S}*
PATX155	64/F	Pancreatic body tumor	*KRAS^{G12D}, TP53^{P33R}*
PATX110	77/M	Pancreatic head tumor	*KRAS^{G12D}, TP53^{R282W}, CDKN2A^{Y44*}*
PATX53	66/M	Liver metastasis	*KRAS^{G12D}, TP53^{R306*}*
PATX69	64/M	Pancreatic tail tumor	*KRAS^{G12D}, TP53^{N235dup}, CDKN2A^{A102Rfs*44}*
PATX66	64/F	Pancreatic head tumor	*KRAS^{G12D}, TP53^{Y234*}, CDKN2A^{Y44*}*

Table S3: Flow cytometry antibodies. Related to STAR Methods.

Antibody	Clone ID	Dilution	Vendor, catalog number
Anti-mouse CD45-Pacific Blue	30-F11	1:100	Bio Legend, 103126
Anti-mouse CD3-PE-Cy7	145-2C11	1:100	eBioscience, 25-0031-82
Anti-mouse CD4-BV605	RM4-5	1:200	BioLegend, 100548
Anti-mouse CD8-BV650	53-6.7	1:200	BioLegend, 100742
Anti-mouse CD11b-BV711	M1/70	1:400	BD Bioscience, 563168
Anti-mouse F4/80-PE	CI:A3-1	1:50	BioRad, MCA497PE
Anti-mouse CD19-PerCP-Cy5.5	1D3	1:100	BD Bioscience, 561113
Anti-mouse CD11c-PE-CF594	HL3	1:100	BD Bioscience, 562454
Anti-mouse NK1.1, PE	PK136	1:100	eBioscience,12-5941-83

Table S4: Flow cytometry antibodies for FASL analysis. Related to STAR Methods.

Antibody	Clone ID	Dilution	Vendor, catalog number
Anti-mouse CD45-BV510	30-F11	1:200	BioLegend, 103137
Anti-mouse CD11b-BV786	M1/70	1:200	BD Bioscience, 740861
Anti-mouse CD4-BV605	RM4-5	1:200	BioLegend, 100548
Anti-mouse CD8-BV650	53-6.7	1:200	BioLegend, 100742
Anti-mouse CD3-PE-Cy7	145-2C11	1:200	eBioscience, 25-0031-82
Anti-mouse CD178 (FasL)-APC	MFL3	1:100	BioLegend, 106609

Table S5: qPCR primer sequences. Related to STAR Methods.

Gene	Forward primer sequence	Reverse primer sequence
Fas	5’ TATCAAGGAGGCCCATTTTGC 3’	5’ TGTTTCCACTTCTAAACCATGCT 3’
18s	5′ GTAACCCGTTGAACCCCATT 3′	5′ CCATCCAATCGGTAGTAGCG 3′
Gapdh	5’ AGGTCGGTGTGAACGGATTT 3’	5’ TGTAGACCATGTAGTTGAGGTCA 3’
ACTB	5’ AGAAAATCTGGCACCACACC 3’	5’ AGAGGCGTACAGGGATAGCA 3’
FAS	5’ GGACCCAGAATACCAAGTGCAG 3’	5’ GTTGCTGGTGAGTGTGCATTCC 3’

Uncropped blots

Uncropped blots

Figure 1A

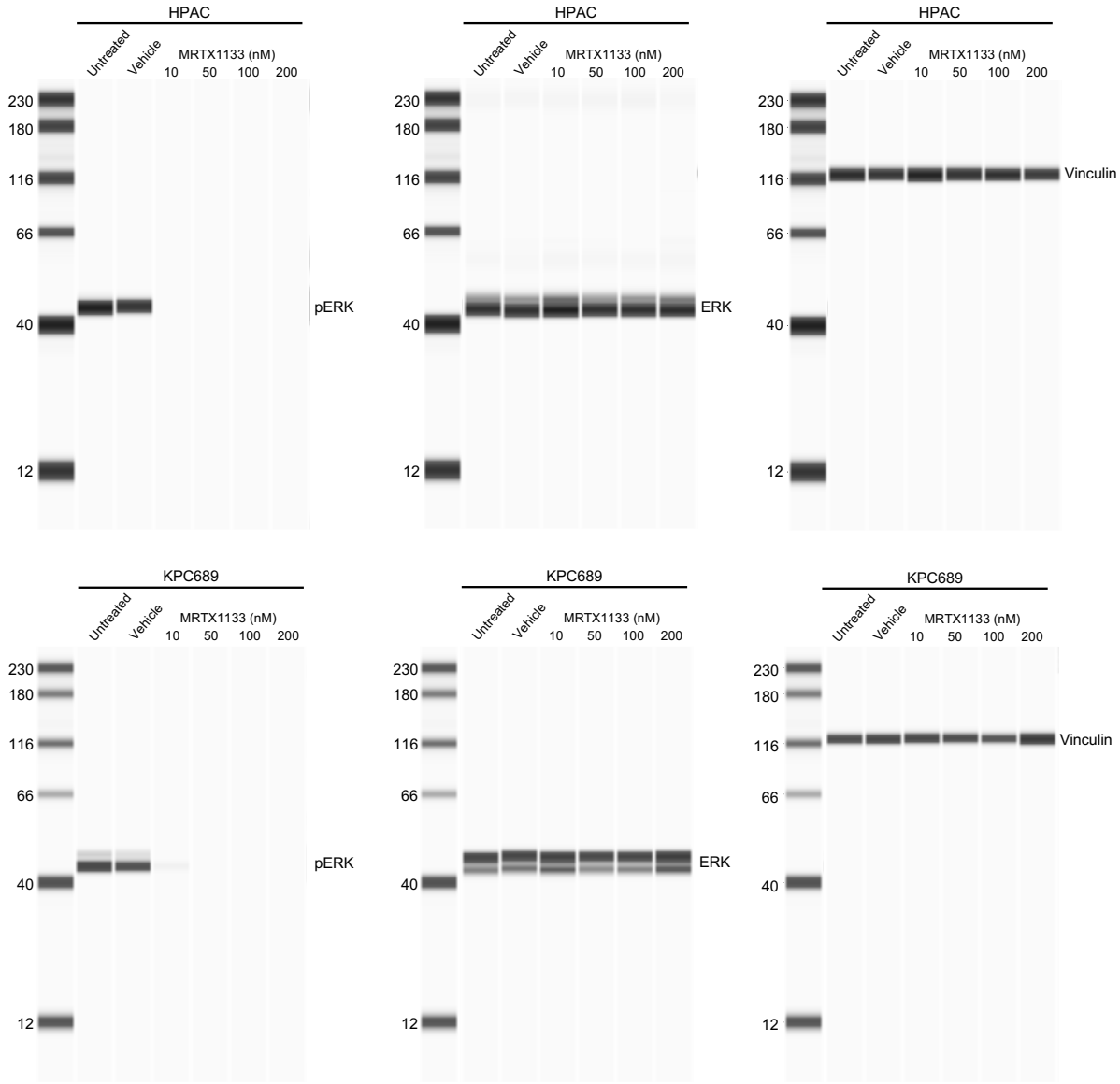

Uncropped blots

Figure 6E

p-ERK
MRTX849
MIA Paca-2

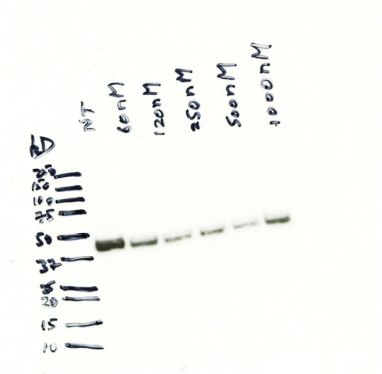

Vinculin
MRTX849
MIA Paca-2

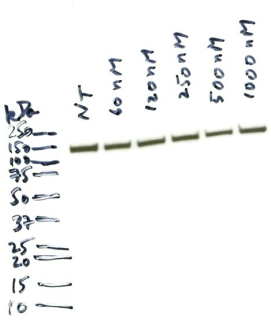

Figure 6J

p-ERK
MRTX1133
DH-50

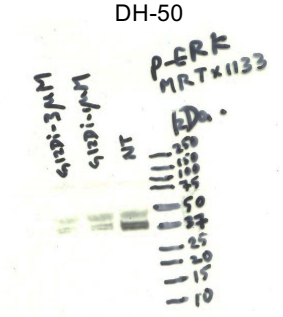

Vinculin
MRTX1133
DH-50

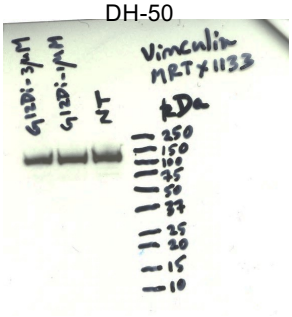

Uncropped blots

Figure 6H

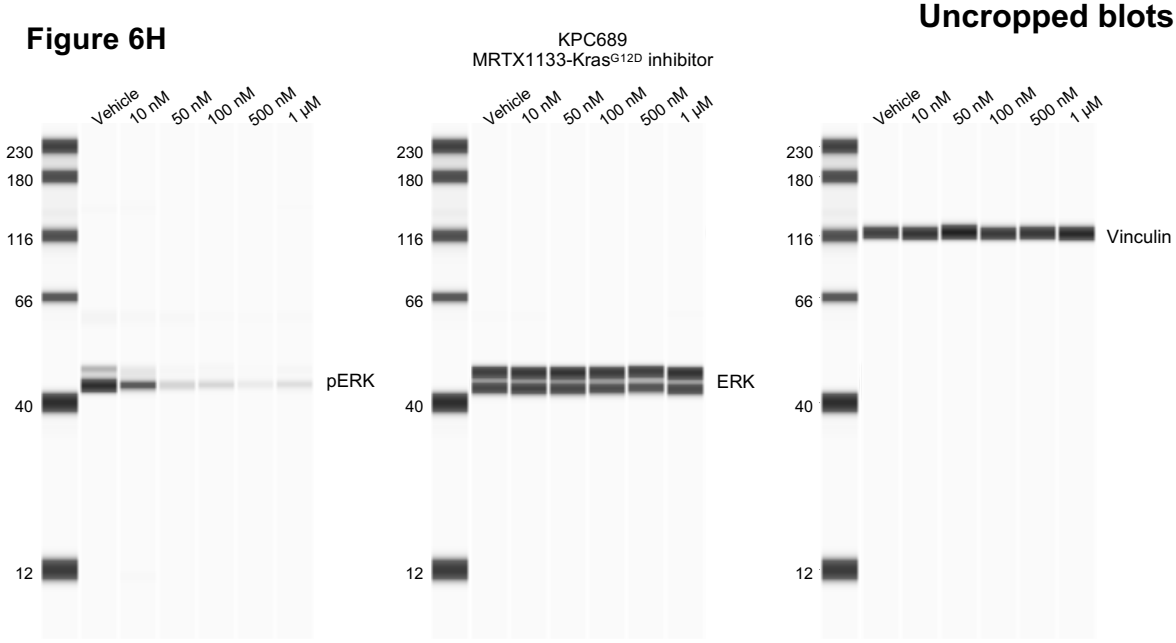

Supplemental Figure 10E

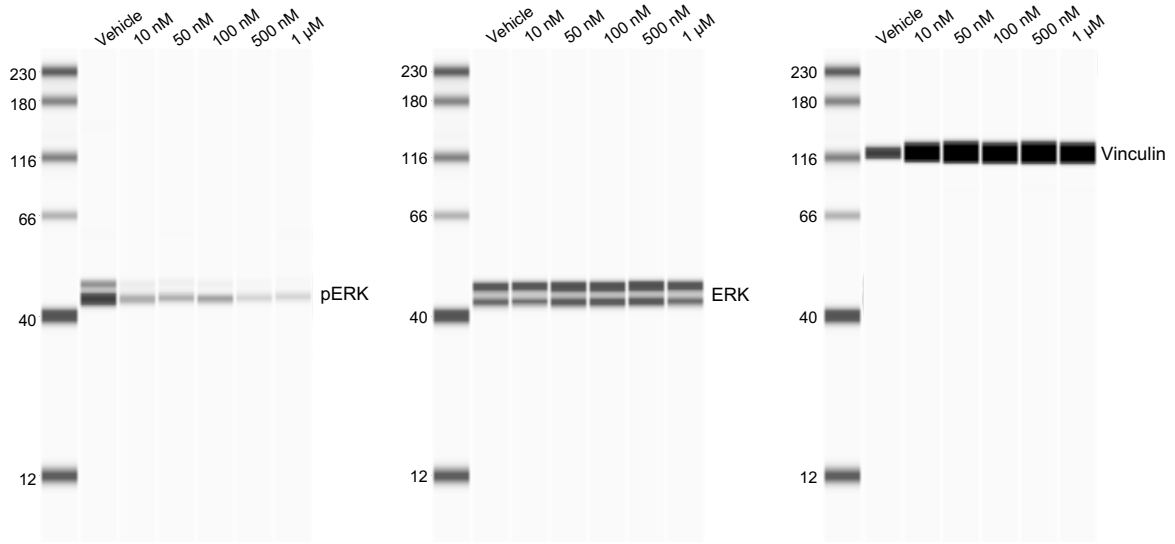

Uncropped blots

Figure S10F